Virchows Arch (2001) 438:192–197
DOI 10.1007/s004280000287

CASE REPORT

**Klaus Kayser · Stefan Zink · Bianca Link
Felix Herth · Hendrik Dienemann · Ludwig Schrod
Hans-Joachim Gabius**

Endobronchial juvenile hemangioma – a case report of a neonate including immunohistochemical monitoring and nuclear, cellular, and vascular morphometry

Received: 1 March 2000 / Accepted: 5 July 2000 / Published online: 1 November 2000

Abstract A 3-month-old female child suffered from tachypnea and dyspnea with abnormal blood gas values. Chest X-rays revealed an increased transparency of the left lung and a mediastinal shift to the right side. High resolution computed tomography (CT) documented a narrowing of the left upper stem bronchus. Ensuing endoscopy detected an occlusive endobronchial tumor mass that did not infiltrate the bronchial cartilage as confirmed with endobronchial ultrasonic monitoring. Based on gross histological examination of the surgical specimen obtained using sleeve resection, the highly vascularized tumor exhibited an adenomatoid growth pattern with a rather homogeneous population of nuclei. The light microscopical presentation was consistent with a juvenile (infantile) hemangioma, which was confirmed using immunohistochemical examinations despite the display of neuroendocrine features. Although endobronchial juvenile hemangiomas are an extremely rare event in early childhood, this case underscores the necessity to not neglect its occurrence in differential diagnosis.

K. Kayser (✉) · S. Zink
Department of Pathology, Thoraxklinik, Amalienstr. 5,
69126 Heidelberg, Germany
e-mail: klkayser@lung.de
Tel.: +49-6221-396496, Fax: +49-6221-396238

B. Link · H. Dienemann
Department of Thoracic Surgery, Thoraxklinik, 69126 Heidelberg, Germany

F. Herth
Department of Bronchoscopy, Thoraxklinik, 69126 Heidelberg, Germany

L. Schrod
Department of Pediatrics, University of Wuerzburg,
97080 Wuerzburg, Germany

H.-J. Gabius
Institute of Physiological Chemistry, University of Munich,
80539 Munich, Germany

Keywords Current of entropy · Juvenile hemangioma · Lung · Morphometry · Sleeve resection

Introduction

Benign and malignant endobronchial tumors in early childhood are extremely rare [11, 21]. They include a broad variety of morphological features, especially carcinoids, blastoma, mucoepidermoid carcinomas, and various kinds of sarcomas, such as leiomyosarcomas or rhabdomyosarcomas [4, 7, 10, 16]. Carcinoid tumors have been described most frequently, although the number of documented cases in childhood hardly exceeds 50 cases. In young children, hemangiomas may arise from various organs. Those originating from the bronchi or lungs have so far been reported only in two instances. One case, demonstrated by Cohen and Kaschula in 1992, was accompanied by a cough, bronchitis, and pneumonia of the right lung and displayed an endobronchial occlusive growth [4]. Additionally, two cases have been described in three-month-old girls in which the hemangiomas arose in the mediastinum and involved the trachea [17]. In neonates, no such tumor originating from the air conduction system has up to now been described to our knowledge. However, infantile hemangiomas are known to occur infrequently in liver, the periparotid region, skin, or all compartments of the mediastinum [2, 3, 8, 9, 20].

In addition to standard case presentation of the juvenile endobronchial hemangioma from the 3-month-old girl, morphometric analysis and the application of a panel of probes enabled us to report further characteristics of this tumor. The Feulgen-stained specimen was used to determine the structural entropy and its current [13, 11]. These parameters have recently been recognized as a reliable prognostic feature in resected common bronchial carcinomas and carcinoids of adults [11, 12, 15]. The evaluation of positivity for the proliferation marker Ki-

67 (MIB-1) yielded insight into the proliferative status, and the profiling of the vascular system, including the average diffusion distance into the tumor vascularization. Further markers included indicators of neuroendocrine functions, immune mediators, and two endogenous lectins with impact on intercellular adhesion, communication, and signaling [1, 5, 6, 14].

Case description

This 3-month-old female infant caused suspicion due to cerebral convulsions and myoclonia and, therefore, was kept under clinical observation for 2 weeks after birth. No organ abnormalities could be delineated, and the infant was released from hospital. At the age of 3 months, the child suffered from increasing dyspnea and tachypnea and was again hospitalized. The chest X-ray (Fig. 1) displayed a decreased density of the left lung and a mediastinal shift to the right side. No response in therapeutic attempts with bronchodilators (euphyllin) could be noted. High-resolution computed tomography (CT) revealed a significant narrowing of the left main-stem bronchus. This was confirmed using bronchoscopy (Fig. 2). Endobronchial inspection with ultrasound gave evidence for a tumor mass occupying the submucosal tissue extending to the bronchial cartilage (Fig. 3). Blood gas analysis data were as follows: arterial tensions (pO_2) 52 mmHg, (pCO_2) 35 mmHg; pH 7.42; base excess (BE) 0.6 mmol/l; standard bicarbonate (StBic) 23.8 mmol/l. Blood and serum values were within the normal range.

One week later, a complete tumor resection was performed with re-anastomosis of the main-stem bronchus. Unsuspicious post-surgical follow-up with complete revascularization of the main bronchus and normal wound healing followed, accompanied by a normalization of blood gas. The child was discharged 2 weeks after hospitalization.

Morphological findings

The excised tumor measured 5×5×5 mm in maximum diameters and was of soft to firm consistence. Macroscopically, the tumor occupied more than 80% of the lumen of the left main-stem bronchus and was of red to yellowish color. The surface was covered by rather normally appearing bronchus mucosa (Fig. 4). Intraoperatively, clear resection boundaries on both sides (confirmed by frozen-section analysis) were obtained.

Microscopically, the tumor was characterized by a dense network of capillaries and larger vessels, locally forming venous ectasia (Fig. 5). The tumor cell population displayed only a small extent of variation in shape and size of nuclei and cytoplasm. Fine and coarsely distributed nuclear chromatin was seen, and mitoses were difficult to note. The majority of tumor cells was closely connected to the intra-tumorous vascular walls and formed intra-connective clusters when examined using the periodic acid–Schiff (PAS) stain (not shown) without clear-cut neuroendocrine textures. Immunohistochemistry revealed a strong staining for vimentin and CD34 (Fig. 6). Pan-keratin, synaptophysin, and bombesin stains were negative. Further immunohistochemical analysis revealed an expression of galectin-1 and galectin-8.

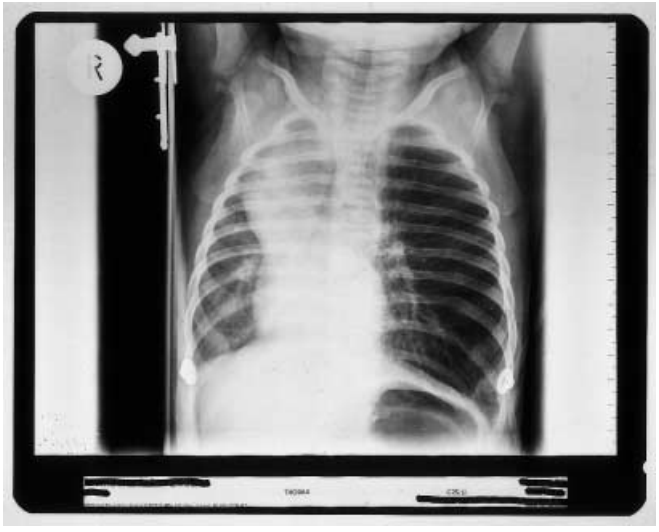

Fig. 1 Chest X-ray showing a mediastinal shift to the right side and decreased density of the left lung side

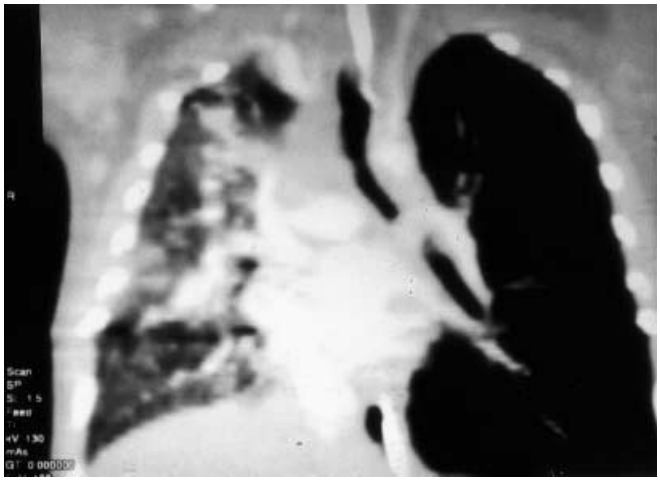

Fig. 2 High-resolution computed tomography showing a narrowing of the left stem bronchus

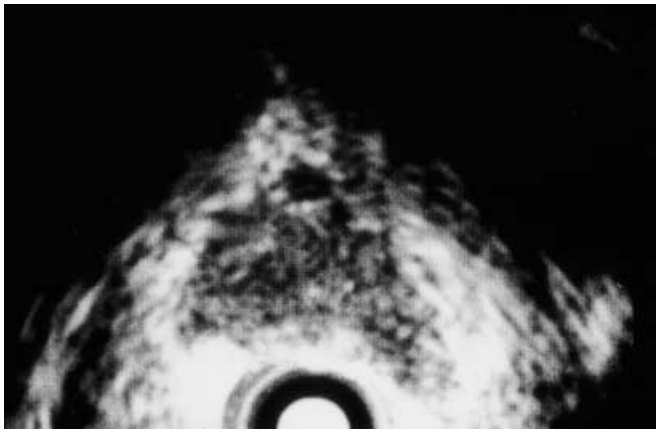

Fig. 3 Endobronchial ultra sound showing a homogeneous mass of the bronchus without infiltration of the bronchial cartilage

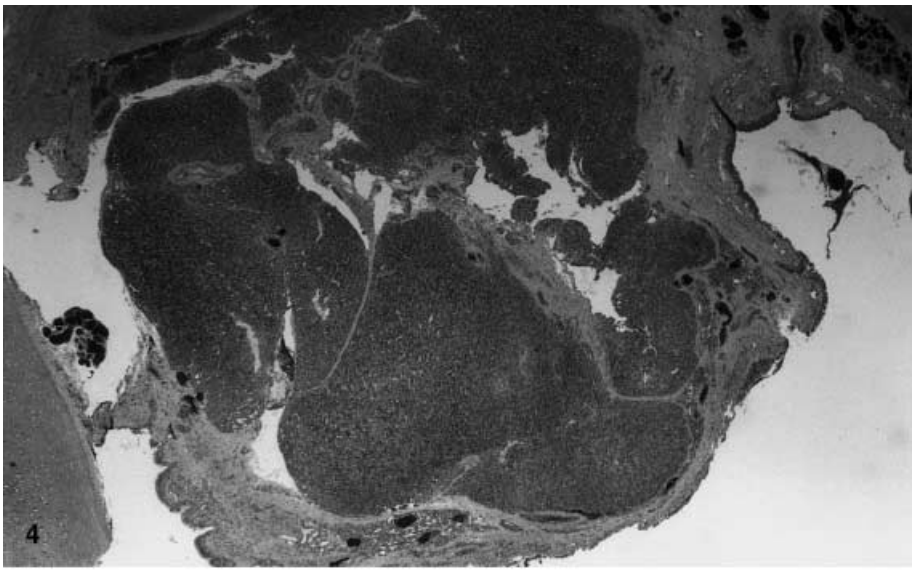

Fig. 4 Microphotograph of the tumor showing an exophytic tumor mass within the left stem bronchus (hematoxylin and eosin, ×16)

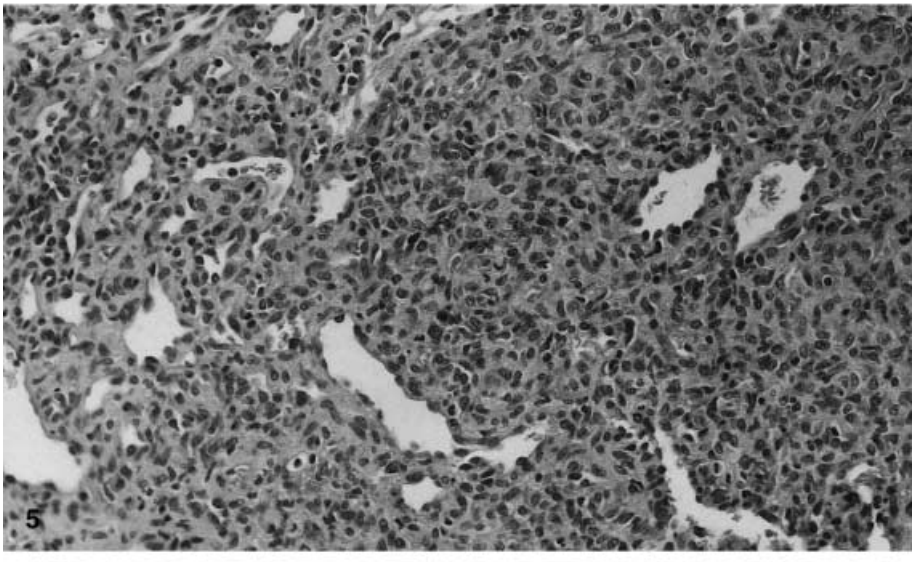

Fig. 5 Microphtograph of the tumor showing a highly vascularized tumor with moderate variation of tumor nuclei and cells in size and shape (hematoxylin and eosin, ×280)

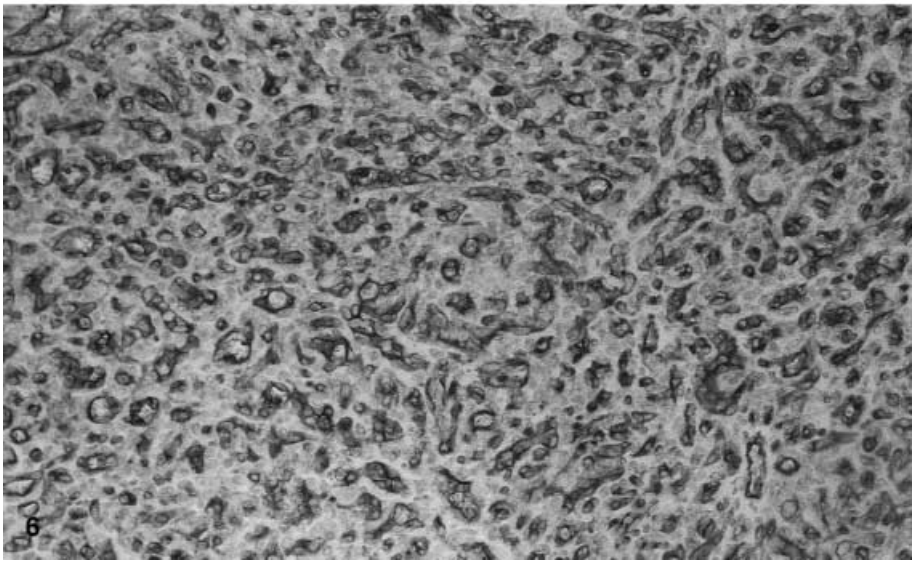

Fig. 6 Microphotograph of the tumor showing a positive immunostaining of tumor cells and vessels to the antibody against CD34 (×280)

The quantitative data of the immuno- and ligandohistochemical investigations are given in Table 1, Table 2, Table 3, Table 4, Table 5, 6 and Table 7. The proliferation index measured by Ki-67 amounted to 3% with a low degree of cluster formation of proliferating and resting tumor cells (Table 1). The static DNA analysis revealed a tetraploid tumor with a low S-phase-related tumor cell fraction and a low structural [minimum spanning tree (MST)] entropy and current of structural entropy (Table 2). The mean diffusion distance measured 6 µm, a short distance when compared with ordinary lung cancer features (Table 3). The expression of the growth-regulating homodimeric and tandem-repeat galectins was moderate to strong (Table 4 and Tables 5, 6). Also, an immune regulator (the lymphokine macrophage migration inhibitory factor) and calcyclin, another member of the S100-protein family (S100A6), were present in the tumor. Remarkably, the lymphokine's presence in bronchial carcinomas is an indicator of favorable prognosis [12]. The entropy and current of entropy are small relative to data of common lung carcinomas and reflect the "homogeneous nature" of the tumor, with a dense capillary network providing the tumor with a large inner energy-exchange surface (Table 7).

Table 1 Proliferation properties measured by (Ki-67)-immunohistochemistry

Percentage of nuclear area of tumor cells	41.5%
Positive nuclei	3% (11/285 nuclei measured)
Area of positive nuclei	1.8%
Distance between	
Positive nuclei	36±53 µm
Negative nuclei	9±5 µm
Positive-negative nuclei	8±1 µm
Cluster formation	
Positive cells	
Cluster radius 106±8 µm	Number of tumor cells/cluster 4±2
Negative cells	
Cluster radius 177±17 µm	Number of tumor cells/cluster 90±24

Table 2 Integrated optical density and syntactic structure analysis

Tetraploid tumor	Peaks at 2.0°C and 4.0°C
S-phase-related fraction	3.8%
Distance between tumor cells	29±18 µm
Distance lymphocyte-tumor cell	14±6 µm
Structural entropy	90
Current of structural entropy	2.4×10^{-3} µm^{-2}

Table 3 Tumor vascularization

Vascular area	118±71 µm^2
Vascular circumference	37±11 µm
Minimum diameter	8±3 µm
Surface/area fraction length area	5.3%
Area fraction	24%
Average diffusion length	6±6 µm

Table 4 Quantitation of staining intensities of tumor cells (as percentage of tumor cells) (*MIF* macrophage migration inhibitory factor)

Probe	Staining intensity		
	Negative	Moderate	Strong
Vimentin	9.7	70.3	20.0
Galectin-1	27.0	71.0	2.0
Galectin-8	42.5	56.0	1.5
Calcyclin	24.5	75.5	0.0
MIF	22.7	70.0	7.3

Table 5 Distances of tumor cells with respect to their staining intensity (in µm)

Probe	Staining intensity		
	Negative	Moderate	Strong
Vimentin	30	12	20
Galectin-1	18	12	71
Galectin-8	14	11	51
Calcyclin	14	8	–
MIF	19	12	29

Table 6 Cluster formation of tumor cells with respect to their staining intensity. The cells represent the number of cells per detectable cluster number of cells per detectable cluster

Probe	Staining intensity					
	Negative		Moderate		Strong	
	Radius (µm)	Cells	Radius (µm)	Cells	Radius (µm)	Cells
Vimentin	–	–	46	2.3	21	4
Galectin-1	–	–	23	7.3	–	–
Galectin-8	30	2	23	6.5	–	–
Calcyclin	34	3.5	25	6	–	–
MIF	64	1.7	33	4.2	–	–

Table 7 Structural entropy and current of entropy (E/μm^{-2}) of applied probes

Probe	Entropy	Current of entropy (μm^{-2})[a]
Vimentin	127	5.3×10^{-3}
Galectin-1	125	5.2×10^{-3}
Galectin-8	129	5.5×10^{-3}
Calcyclin	125	5.2×10^{-3}
MIF	127	5.3×10^{-3}

[a] Calculated according to [12]

Discussion

Juvenile hemangiomas form a rare and benign tumor entity in early childhood. They represent an immature form of a capillary hemangioma, and practically all tumors developing at certain sites will be detected before 1 year of age [21]. On average, the liver, the cheeks, the mediastinum, and the periparotid region are common sites of tumor development [21]. In a series of 18 cases of mediastinal hemangiomas, Moran and Suster reported five cases of young children (at or below the age of 2 years) in which the tumors were all located within the anterior mediastinum. Interestingly, 4 of 5 tumors were of the capillary type, and only one related to a cavernous hemangioma [19]. The authors distinguish capillary hemangiomas from cavernous hemangiomas [19]. Capillary hemangiomas were characterized with a lobular growth pattern and with a high proliferation rate of tumor cells which seemed to compress the vascular lumens of the capillaries [19]. The cellular atypias were limited, and mitoses were only occasionally encountered. All of these features fit to the histological appearance of the case described. The second group, comprising the cavernous hemangiomas and only found in adults, displayed ectopic vessels which were separated by broad bands of fibroconnective tissue [19]. Within the entity of primary bronchial tumors in childhood, reports are confined currently to three related cases from Meade et al. [18]. These patients were comprised of three boys at the age of 10, 11, and 16 years, who suffered from peripherally localized hemangiopericytomas. Bowyer and Sheppard [2] reported an additional interesting case of a 1-year old girl. The child was ventilated for a respiratory distress syndrome causing a pseudocyst of the lung. One year later, a capillary hemangioma was seen at the boundary of the pseudocyst [2]. Additional pulmonary entities of these rare childhood tumors comprise carcinoids, mucoepidermoid tumors, myoblastomas (granular cell tumors), bronchial adenomas, fibromas including neurofibromas, and hamartomas [10, 11, 21]. Children suffering from these tumors are generally at the age of 3–10 years or older [4].

Histologically, juvenile hemangiomas have a characteristic texture and cellular size, which can be clearly separated from cavernous hemangiomas and resemble those of a hemangiopericytoma. However, in contrast to hemangiopericytoma, the occurrence of polygonal, plump cells with a fairly high number of mitoses is frequent. The reticulin (or PAS) stain usually labels clusters of cells and not individual cells as seen in hemangiopericytoma. In addition, cells lying within the reticulin fibers match with those outside these fibers, because all of them are of endothelial origin. The lesions are clearly benign and may even regress without any treatment. Sleeve resection is the most appropriate treatment for endobronchial benign tumors in the childhood, provided a frozen section service can ascertain clear resection boundaries intraoperatively [7, 22], as unambiguously seen even in this infant.

Our patient suffered from rapidly developing symptoms related to a rapid narrowing of a major bronchus. Within a couple of weeks, the child developed severe tachypnea and dyspnea with an inspiration frequency of 100 breaths per minute. Consecutively, the oxygen pressure decreased to 52 mmHg, and that of CO_2 increased. The tumor was detected using endoscopy, revealing a firm endobronchial lesion with a normal epithelial surface. Histologically, the tumor harbored the characteristics of a juvenile hemangioma, which was confirmed using immunohistochemistry. Interestingly, a weak expression of a member of the S100-protein family (calcyclin, S100A6) was detected, whereas other neuroendocrine markers (bombesin, synaptophysin) failed to stain positively. About 40% of the tumor volume was occupied by tumor cell nuclei, and 1.8% of the total tumor volume (area/area fraction) corresponds to proliferating tumor cells. The proliferating 3% of tumor cells, which is in close agreement with the S-phase-fraction of 3.8% measured using static DNA analysis, formed clusters of four tumor cells at average and a cluster radius of 106 μm. The clusters formed by non-proliferating tumor cells contained 90 cells with a mean cluster radius of 177 μm (Table 1). The results of the quantitative staining of the probes vimentin, galectin-1, galectin-8, calcyclin, and macrophage migration inhibitory factor (MIF), given in Table 4, demonstrate that only a minority of tumor cells possess a high antigen density. The tumor is highly vascularized, and about 24% of the tumor volume can be ascribed to vessels. The average diffusion length, which is the mean distance of a tumor cell from its nearest vessel, amounts to only 6 μm, which is about 10% of that of a common bronchial carcinoma [13]. Conventional immunohistochemistry of our case is in accordance with data obtained from examination of infantile hemangiomas occurring in the liver or skin. Ceraret al. [2] reported the detection of vimentin, von Willebrand factor, CD31, *Ulex europaeus* agglutinin-reactive glycoconjugates, and α-smooth muscle actin. Similar results were obtained from Gonzalez-Crussiand Reyes-Mugica [9] who could, in addition, detect an interstitially located cell, which was positive for a macrophage marker in a series of 10 cases. Our case was strongly positive to CD34 and vimentin.

In summary, albeit very rare, a benign tumor entity of an infantile hemangioma can occur in the bronchus. It should be excised using sleeve resection, allowing an apparently normal lung development, as documented by the clinical follow-up.

Acknowledgements We are grateful for financial support from Dr. M. Scheel-Stiftung für Krebsforschung and the Verein zur Förderung des biologisch-technologischen Fortschritts in der Medizin e.V.

References

1. André S, Kojima S, Yamazaki N, Fink C, Kaltner H, Kayser K, Gabius HJ (1999) Galectins-1 and -3 and their ligands in tumor biology. J Cancer Res Clin Oncol 125:461–474
2. Bowyer JJ, Sheppard M (1990) Capillary hemangioma presenting as a lung pseudocyst. Arch Dis Child 65:1162–1164
3. Cerar A, Dolenc-Strazar Z (1996) Infantile hemangioendothelioma of the liver in a neonate. Immunohistochemical observations. Am J Surg Pathol 20:871–876
4. Cohen M, Kaschula ROC (1992) Primary tumors in childhood: a review of 31 years' experience and the literature. Pediatric Pulmonol 140:222–232
5. Gabius HJ (1997) Animal lectins. Eur J Biochem 243:543–576
6. Gabius HJ (1997) Concepts of tumor lectinology. Cancer Invest 15:454–464
7. Gaissert HA, Mathisen DJ, Grillo HC, Vacanti JP, Wain JC (1994) Tracheobronchial sleeve resection in children and adolescents. J Pediatric Surg 29:192–198
8. Goldman R, Perzik S (1969) Infantile hemangioma of the parotid gland: a clinicopathological study of 15 cases. Arch Otolaryngol 90:605–608
9. Gonzalez-Crussi F, Reyes-Mugica M (1991) Cellular hemangiomas ("hemangioendotheliomas") in infants. Am J Surg Pathol 15:769–778
10. Hartman GE, Shochat SJ (1983) Primary pulmonary neoplasms of childhood: a review. Ann Thoracic Surg 36:108–119
11. Kayser K (1992) Analytical lung pathology, Springer, Berlin Heidelberg New York
12. Kayser K, Gabius HJ (1997) Graph theory and the entropy concept in histochemistry. Progr Histochem Cytochem 32: 1–106
13. Kayser K, Gabius HJ (1999) The application of thermodynamic principles to histochemical and morphometric tissue research: principles and practical outline with focus on the glycosciences. Cell Tissue Res 296:443–455
14. Kayser K, Bovin NV, Korchagina EY, Zeilinger C, Zeng FY,Gabius HJ (1994) Correlation of expression of binding sites for synthetic blood group A-, B- and H-trisaccharides and for sarcolectin with survival of patients with bronchial carcinoma. Eur J Cancer 30:653–657
15. Kayser K, Kayser C,Rahn W, Bovin NV, Gabius HJ (1996) Carcinoid tumor of the lung: immuno- and ligandohistochemistry, analysis of integrated optical density, syntactic structure analysis, clinical data, and prognosis of patients treated surgically. J Surg Oncol 63:99–106
16. Lack EE, Harris GB, Eraklis A, Vawter GF (1983) Primary bronchial tumors in childhood. Cancer 51:492–497
17. Messineo A, Wesson DE, Filler RM, Smith CR (1992) Juvenile hemangiomas involving the thoracic trachea in children: report of two cases. J Pediatr Surg 27:1291–1293
18. Meade JB, Whitwell F, Bickford BJ, Waddingston JKB (1974) Primary hemangiopericytoma of the lung. Thorax 29:1–6
19. Moran CA, Suster S (1995) Mediastinal hemangiomas: a study of 18 cases with emphasis on the spectrum of morphological features. Hum Pathol 26:416–421
20. Nagao K, Masuzaki O, Shigematsu H, Kaneko T, Katoh T, Kitamura T (1984) Histopathologic studies of benign infantile hemangioendothelioma of the parotid gland. Mayo Clin Proc 59:3–11
21. Sternberg S (1994) Diagnostic surgical pathology. (vol 1) Raven Press, New York
22. Tischer W, Reddmann H, Herzog P, Gdanietz K, Witt J, Wurnig P, Reiner A (1985) Experience in surgical treatment of pulmonary and bronchial tumors in childhood. Prog Pediatr Surg 21:119–135